Institute of Structural Mechanics and
Dynamics in Aerospace Engineering

Univ.-Prof. Dr.-Ing. Tim Ricken

Simulation of Coupled Problems with the Finite Element Method

Group 2

Non-linear Thermo-elasticity

Adinath Shirodkar 3702813

Ganesh Vasant Terve 3766778

Institute of Structural Mechanics and Dynamics in Aerospace Engineering (ISD)
University of Stuttgart
Summer Semester 2025

Contents

September 21, 2025

1 Derivation of Piola-Kirchhoff Stress Tensors from Helmholtz Free Energy

We derive the second and first Piola-Kirchhoff stress tensors $\mathbf{S}$ and $\mathbf{P}$ from the Helmholtz free energy function:

$$\begin{aligned}\rho_0\Psi &= \alpha_1(J^{-2/3}I_C - 3) + \alpha_2(J^{-4/3}II_C - 3) + \frac{\alpha_3}{2}(J-1)^2 \\ &\quad - \rho_0\beta\,\ln(J)\,(\theta-\theta_0)\; - \rho_0 c_\varepsilon\left(\theta\ln\frac{\theta}{\theta_0} - \theta + \theta_0\right)\end{aligned}$$

Here:

- $I_C = \mathrm{tr}(\mathbf{C})$ is the first invariant
- $II_C = \frac{1}{2}(I_C^2 - \mathrm{tr}(\mathbf{C}^2))$ is the second invariant
- $J = \sqrt{\det\mathbf{C}}$ is the volume change
- $\mathbf{C} = \mathbf{F}^T\mathbf{F}$ is the right Cauchy-Green deformation tensor

1.1 Derivatives of Invariants with Respect to $\mathbf{C}$

$$\begin{aligned}\frac{\partial I_C}{\partial\mathbf{C}} &= \mathbf{I} \\ \frac{\partial II_C}{\partial\mathbf{C}} &= I_C\mathbf{I} - \mathbf{C} \\ \frac{\partial J}{\partial\mathbf{C}} &= \frac{1}{2}J\mathbf{C}^{-1}\end{aligned}$$

1.2 Derivatives of Free Energy with Respect to Invariants

$$\begin{aligned}\rho_0\frac{\partial\Psi}{\partial I_C} &= \alpha_1 J^{-2/3} \\ \rho_0\frac{\partial\Psi}{\partial II_C} &= \alpha_2 J^{-4/3} \\ \rho_0\frac{\partial\Psi}{\partial J} &= -\frac{2}{3}\alpha_1 J^{-5/3}I_C - \frac{4}{3}\alpha_2 J^{-7/3}II_C + \alpha_3(J-1) - \frac{\beta(\theta-\theta_0)}{J}\end{aligned}$$

1.3 Derivative of Ψ with Respect to $\mathbf{C}$

$$\rho_0\frac{\partial\Psi}{\partial\mathbf{C}} = \frac{\partial\Psi}{\partial I_C}\frac{\partial I_C}{\partial\mathbf{C}} + \frac{\partial\Psi}{\partial II_C}\frac{\partial II_C}{\partial\mathbf{C}} + \frac{\partial\Psi}{\partial J}\frac{\partial J}{\partial\mathbf{C}}$$

$$\begin{aligned}\rho_0\frac{\partial\Psi}{\partial\mathbf{C}} &= \alpha_1 J^{-2/3}\mathbf{I} + \alpha_2 J^{-4/3}(I_C\mathbf{I} - \mathbf{C}) \\ &\quad + \left(-\frac{1}{3}\alpha_1 J^{-2/3}I_C - \frac{2}{3}\alpha_2 J^{-4/3}II_C + \frac{\alpha_3}{2}J(J-1) - \frac{1}{2}\beta(\theta-\theta_0)\right)\mathbf{C}^{-1}.\end{aligned} \tag{1}$$

1.4 Second Piola-Kirchhoff Stress Tensor $\mathbf{S}$

$$\begin{aligned}\mathbf{S} &= 2\rho_0\frac{\partial\Psi}{\partial\mathbf{C}} \\ &= 2\Bigg[\left(\alpha_1 J^{-2/3} + \alpha_2 J^{-4/3}I_C\right)\mathbf{I} - \alpha_2 J^{-4/3}\mathbf{C} \\ &\quad + \left(-\frac{1}{3}\alpha_1 J^{-2/3}I_C - \frac{2}{3}\alpha_2 J^{-4/3}II_C + \frac{\alpha_3}{2}J(J-1) - \frac{1}{2}\beta(\theta-\theta_0)\right)\mathbf{C}^{-1}\Bigg]\end{aligned}$$

1.5 First Piola-Kirchhoff Stress Tensor $\mathbb{P}$

Using the identity $\mathbf{P} = \mathbf{FS}$, and relations:

$$\mathbf{C} = \mathbf{F}^T\mathbf{F}, \quad \mathbf{C}^{-1} = \mathbf{F}^{-1}\mathbf{F}^{-T}, \quad \mathbf{FC}^{-1} = \mathbf{F}^{-T}$$

The first Piola-Kirchhoff stress tensor becomes:

$$\begin{aligned} \mathbf{P} = 2\Bigg[& \left(\alpha_1 J^{-2/3} + \alpha_2 J^{-4/3} I_C\right)\mathbf{F} \; - \; \alpha_2 J^{-4/3}\mathbf{FC} \\ & + \; \left(-\frac{1}{3}\alpha_1 J^{-2/3} I_C - \frac{2}{3}\alpha_2 J^{-4/3} II_C + \frac{\alpha_3}{2} J(J-1) - \frac{1}{2}\beta(\theta - \theta_0)\right)\mathbf{F}^{-T}\Bigg]. \end{aligned} \tag{2}$$

2 Strong Forms of the Nonlinear Thermo-Mechanical Problem in Reference Configuration

We now derive the strong form equations for a coupled thermo-mechanical problem in the reference configuration. The analysis assumes no body forces and no heat sources.

2.1 Balance of Mass

For mass conservation, the mass of any material volume must remain constant over time. This implies:

$$\dot{m} = 0$$

An infinitesimal mass element in the current configuration $dm(\mathbf{x}) = \rho\, dv$ must equal that in the reference configuration $dm(\mathbf{X}) = \rho_0\, dV$. Here, ρ_0 and ρ are the mass densities in the reference and current configurations, respectively. The continuity equation in the spatial description is:

$$\dot{\rho} + \rho\, \mathrm{div}(\dot{\mathbf{x}}) = 0 \tag{3}$$

This ensures conservation of mass throughout the motion.

2.2 Balance of Linear Momentum

Step 1: General Strong Form The spatial (current configuration) form of the linear momentum equation is:

$$\rho\ddot{\mathbf{x}} = \rho\mathbf{b} + \mathrm{div}(\mathbf{T}) \tag{4}$$

Step 2: Quasi-Static Assumption Neglecting inertial effects ($\ddot{\mathbf{x}} = 0$) gives:

$$0 = \rho\mathbf{b} + \mathrm{div}(\mathbf{T}) \tag{5}$$

Step 3: No Body Forces Assuming $\mathbf{b} = 0$, we obtain:

$$\mathrm{div}(\mathbf{T}) = 0 \tag{6}$$

Step 4: Transformation to Reference Configuration Using the Piola transformation and the relation $\mathbf{T} = J^{-1}\mathbf{P}\mathbf{F}^T$, the divergence theorem gives:

$$\int_{\Omega_t} \mathrm{div}\,\mathbf{T}\, dv = \int_{\partial\Omega_t} \mathbf{T}\cdot\mathbf{n}\, da = \int_{\partial\Omega_0} \mathbf{P}\cdot\mathbf{N}\, dA = \int_{\Omega_0} \mathrm{Div}\,\mathbf{P}\, dV \tag{7}$$

Step 5: Final Strong Form The balance of linear momentum in the reference configuration becomes:

$$\boxed{\int_{\Omega_0} \mathrm{Div}\,\mathbf{P} dV = \mathbf{0}} \tag{8}$$

2.3 Balance of Energy

Step 1: Spatial Form The spatial form of the energy equation is:

$$\int_{\Omega_t} \rho c_\varepsilon \dot{\theta}\, dv + \int_{\Omega_t} \frac{\beta\theta}{J} \mathrm{grad}(\dot{\mathbf{x}}) : \mathbf{I}\, dv - \int_{\Omega_t} \mathrm{div}(\mathbf{q})\, dv = 0 \tag{9}$$

Step 2: Mapping to Reference Configuration Use the transformations:

$$\begin{aligned} \rho &= \rho_0 / J \\ dv &= J\, dV \\ \mathrm{div}\, \mathbf{q} &= J^{-1} \mathrm{Div}\, \mathbf{Q}, \quad \text{with } \mathbf{Q} = J\mathbf{F}^{-1}\mathbf{q} \end{aligned}$$

Step 3: Final Strong Form in Reference Configuration The energy equation becomes:

$$\boxed{\int_{\Omega_0} \rho_0 c_\varepsilon \dot{\theta}\, dV + \int_{\Omega_0} \beta\theta\, \mathrm{Grad}(\dot{\mathbf{x}}) : \mathbf{F}^{-T}\, dV + \int_{\Omega_0} \mathrm{Div}(\mathbf{Q})\, dV = 0} \tag{10}$$

The heat flux in reference configuration is given by:

$$\mathbf{Q} = -kJ\mathbf{C}^{-1} \mathrm{Grad}\, \theta$$

This completes the strong form derivation for the mass, momentum, and energy balances in the reference configuration.

2.4 Weak Form of Linear Momentum

Starting from Equation (8), the weak form is obtained using the Galerkin procedure. We multiply the strong form by a vector-valued test function $\delta\mathbf{u}$ vanishing on $\partial\Omega_0^u$:

$$\int_{\Omega_0} \mathrm{Div}\, \mathbf{P} \cdot \delta\mathbf{u}\, dV = 0 \tag{11}$$

Boundary Conditions

$$\begin{aligned} \mathbf{u} &= \bar{\mathbf{u}} \quad \text{on } \partial\Omega_0^u \\ \mathbf{P} \cdot \mathbf{N} &= \bar{\mathbf{t}} \quad \text{on } \partial\Omega_0^t \end{aligned}$$

Function Space

$$\delta\mathbf{u} \in H_0^1(\Omega_0) = \{\mathbf{v} \in H^1(\Omega_0) : \mathbf{v} = 0 \text{ on } \partial\Omega_0^u\}$$

Integration by Parts Using the identity:

$$(\mathrm{Div}\, \mathbf{P}) \cdot \delta\mathbf{u} = \mathrm{Div}(\mathbf{P}^T \cdot \delta\mathbf{u}) - \mathbf{P} : \mathrm{Grad}\, \delta\mathbf{u}$$

we obtain:

$$\int_{\Omega_0} \mathbf{P} : \mathrm{Grad}\, \delta\mathbf{u}\, dV = \int_{\partial\Omega_0} \bar{\mathbf{t}} \cdot \delta\mathbf{u}\, dA \tag{12}$$

Weak Form Residuum

$$R_u = \int_{\Omega_0} \mathbf{P} : \mathrm{Grad}\, \delta\mathbf{u}\, dV - \int_{\partial\Omega_0} \bar{\mathbf{t}} \cdot \delta\mathbf{u}\, dA \tag{13}$$

Using $\mathbf{P} = \mathbf{F} \cdot \mathbf{S}$, we can also express the weak form in terms of Green-Lagrange strain:

$$\boxed{R_u = \int_{\Omega_0} \mathbf{S} : \delta\mathbf{E}\, dV - \int_{\partial\Omega_0} \bar{\mathbf{t}} \cdot \delta\mathbf{u}\, dA = 0} \tag{14}$$

2.5 Weak Form of Energy Balance

In the reference configuration, the strong form of the energy balance is:

$$\int_{\Omega_0} \rho_0 C_\varepsilon \dot{\theta}\, dV + \int_{\Omega_0} \beta\theta\, \mathrm{Grad}(\dot{\mathbf{x}}) \cdot \mathbf{F}^{-T}\, dV + \int_{\Omega_0} \mathrm{Div}(\mathbf{Q})\, dV = 0 \tag{15}$$

where $\mathbf{Q} = -kJ\mathbf{C}^{-1}\mathrm{Grad}\,\theta$.

Step 1: Multiply by Scalar Test Function $\delta\theta$

$$\delta_\theta \in H_0^1(\Omega_0) = \{v \in H^1(\Omega_0) : v = 0 \text{ on } \partial\Omega_0^\theta\}$$

Step 2: Multiply the Strong Form by $\delta\theta$

$$R_\theta = \int_{\Omega_0} \rho_0 C_\varepsilon \dot{\theta}\, \delta_\theta\, dV + \int_{\Omega_0} \beta\theta\, \mathrm{Grad}(\dot{\mathbf{x}}) \cdot \mathbf{F}^{-T}\, \delta_\theta\, dV + \int_{\Omega_0} \mathrm{Div}(\mathbf{Q})\, \delta_\theta\, dV \tag{16}$$

Step 3: Integration by Parts on Heat Conduction Term Using the identity:

$$\mathrm{Div}(\mathbf{Q}\,\delta_\theta) = \mathrm{Div}(\mathbf{Q})\,\delta_\theta + \mathbf{Q} \cdot \mathrm{Grad}(\delta_\theta) \tag{17}$$

gives:

$$\mathrm{Div}(\mathbf{Q}\,\delta_\theta) = \mathbf{Q} \cdot \mathbf{N}\,\delta_\theta\, dA + \mathbf{Q} \cdot \mathrm{Grad}(\delta_\theta) \tag{18}$$

Final Weak Form Residuum

$$\boxed{R_\theta = \int_{\Omega_0} \rho_0 C_\varepsilon \dot{\theta}\, \delta_\theta\, dV - \int_{\Omega_0} \mathbf{Q} \cdot \mathrm{Grad}(\delta_\theta)\, dV + \int_{\Omega_0} \beta\theta\, \mathrm{Grad}(\dot{\mathbf{x}}) \cdot \mathbf{F}^{-T}\, \delta_\theta\, dV + \int_{\partial\Omega_0} \mathbf{Q} \cdot \mathbf{N}\,\delta_\theta\, dA = 0} \tag{19}$$

3 Tangent Operators for the Thermo-Mechanical Coupled Problem

3.1 Linearization of Balance of Momentum R_u

Linearisation of $R(u)$ around a current approximation $\mathbf{u^k}$

$$R_u(\mathbf{u}, \theta, v_u) \approx R(u^k, \theta, v_u) + \left.\frac{\partial R}{\partial u}\right|_{u^k} \cdot \Delta u^{k+1} \tag{20}$$

The weak form of Linear Momentum is given by :

$$R_u(\mathbf{u}, \theta, v_u) = \int_{\Omega_0} \mathbf{S} : \delta \mathbf{E} \, dV - \int_{\partial\Omega_0} \bar{t} : v_u \, dA = 0 \tag{21}$$

$$\mathrm{Lin}[R_{\mathrm{u}}] = R(\tilde{\mathbf{u}}, \theta, v_u) + \int_{\Omega_0} \delta\tilde{\mathbf{E}} : \frac{\partial \mathbf{S}}{\partial \mathbf{C}} \Delta \mathbf{C} \, dV + \int_{\Omega_0} \delta\tilde{\mathbf{E}} : \frac{\partial \mathbf{S}}{\partial \theta} \Delta\theta \, dV \tag{22}$$

Considering linearization around $\mathbf{u}^k$ we can write

$$\tilde{\mathbf{u}} = \mathbf{u}^k, \quad \tilde{\mathbf{F}} = \mathbf{F}(\tilde{\mathbf{u}}) = \mathbf{F}(\mathbf{u}^k), \quad \tilde{\mathbf{S}} = \mathbf{S}(\tilde{\mathbf{u}}) = \mathbf{S}(\mathbf{u}^k), \tag{23}$$

$$\Delta \mathbf{C} = 2\,\mathrm{sym}(\mathbf{F}^\top \,\mathrm{Grad}(\Delta \mathbf{u}^{k+1})), \quad \delta\tilde{\mathbf{E}} = \mathrm{sym}(\tilde{\mathbf{F}}^\top \,\mathrm{Grad}(v_u)) \tag{24}$$

Linearization of the residual yields:

$$\boxed{\begin{aligned} \mathrm{Lin}[R_u] = R(\tilde{\mathbf{u}}, \theta, v_u) &+ \int_{\Omega_0} \delta\tilde{\mathbf{E}} : \left.\frac{\partial \mathbf{S}}{\partial \mathbf{C}}\right|_{\tilde{u}} \Delta \mathbf{C} \, dV && (25) \\ &+ \int_{\Omega_0} \mathrm{Grad}(\Delta u^{k+1}) \, \tilde{\mathbf{S}} \, \mathrm{Grad}(v_u) \, dV + \int_{\Omega_0} \delta\tilde{\mathbf{E}} : \left.\frac{\partial \mathbf{S}}{\partial \theta}\right|_{\tilde{u}} \Delta\theta \, dV && (26) \end{aligned}}$$

where

$$R(\tilde{\mathbf{u}}, \theta, v_u) = \int_{\Omega_0} \tilde{\mathbf{S}} : \delta \mathbf{E} \, dV - \int_{\partial\Omega_0} \bar{t} : v_u \, dA \tag{27}$$

3.1.1 Derivative of Second Piola-Kirchhoff Stress Tensor $\mathbf{S}$ with respect to $\mathbf{C}$

Derivative of Second Piola-Kirchhoff Stress Tensor $\mathbf{S}$ with respect to $\mathbf{C}$

The goal is to compute the fourth-order material tangent tensor:

$$\mathbb{C} = \frac{\partial \mathbf{S}}{\partial \mathbf{E}} = 2\frac{\partial \mathbf{S}}{\partial \mathbf{C}}$$

From earlier derivation:

$$\begin{aligned} \mathbf{S} = 2\Big[&\left(\alpha_1 J^{-2/3} + \alpha_2 J^{-4/3} I_C\right)\mathbf{I} - \alpha_2 J^{-4/3}\mathbf{C} \\ &+ \left(-\frac{1}{3}\alpha_1 J^{-2/3} I_C - \frac{2}{3}\alpha_2 J^{-4/3} II_C + \frac{\alpha_3}{2}J(J-1) - \frac{1}{2}\beta(\theta-\theta_0)\right)\mathbf{C}^{-1}\Big] \end{aligned} \tag{28}$$

We define the following terms:

$$\begin{aligned} f_1 &= \alpha_1 J^{-2/3} + \alpha_2 J^{-4/3} I_C \\ f_2 &= \alpha_2 J^{-4/3} C \\ f_3 &= -\frac{1}{3}\alpha_1 J^{-2/3} I_C - \frac{2}{3}\alpha_2 J^{-4/3} II_C + \frac{\alpha_3}{2}J(J-1) - \frac{1}{2}\beta(\theta-\theta_0) \end{aligned}$$

We now compute each contribution to $\frac{\partial \mathbf{S}}{\partial \mathbf{C}}$ term-by-term:

Derivative of f_1 with respect to $\mathbf{C}$ We define:

$$f_1(\mathbf{C}) = \alpha_1 J^{-2/3} + \alpha_2 J^{-4/3}\,\mathrm{tr}(\mathbf{C})$$

First term:

$$\begin{aligned} \frac{\partial}{\partial \mathbf{C}}\left(\alpha_1 J^{-2/3}\right) &= \alpha_1 \cdot \frac{d}{d\mathbf{C}}\left(J^{-2/3}\right) = \alpha_1 \cdot \left(-\frac{2}{3}J^{-5/3}\cdot\frac{\partial J}{\partial \mathbf{C}}\right) \\ &= -\frac{1}{3}\alpha_1 J^{-2/3}\mathbf{C}^{-1} \end{aligned} \tag{29}$$

Second term:

$$\begin{aligned} \frac{\partial}{\partial \mathbf{C}}\left(\alpha_2 J^{-4/3}\,\mathrm{tr}(\mathbf{C})\right) &= \alpha_2\left[\frac{d}{d\mathbf{C}}\left(J^{-4/3}\right)\cdot \mathrm{tr}(\mathbf{C}) + J^{-4/3}\cdot\frac{d}{d\mathbf{C}}\mathrm{tr}(\mathbf{C})\right] \\ &= \alpha_2\left(-\frac{2}{3}J^{-4/3} I_C \mathbf{C}^{-1} + J^{-4/3}\mathbf{I}\right) \end{aligned} \tag{30}$$

Combined result:

$$\boxed{\frac{\partial f_1}{\partial \mathbf{C}} = -\frac{1}{3}\alpha_1 J^{-2/3}\mathbf{C}^{-1} - \frac{2}{3}\alpha_2 J^{-4/3} I_C \mathbf{C}^{-1} + \alpha_2 J^{-4/3}\mathbf{I}} \tag{31}$$

Tensor form for tangent:

$$\boxed{\frac{\partial (f_1 \mathbf{I})}{\partial \mathbf{C}} = \left(\frac{\partial f_1}{\partial \mathbf{C}}\right)\otimes \mathbf{I}} \tag{32}$$

Derivative of f_2 with respect to $\mathbf{C}$ We define:

$$f_2(\mathbf{C}) = \alpha_2 J^{-4/3}\mathbf{C}$$

We use the product rule:

$$\frac{\partial}{\partial \mathbf{C}}(f(\mathbf{C})\cdot\mathbf{C}) = \frac{\partial f}{\partial \mathbf{C}}\otimes \mathbf{C} + f\cdot \mathbb{I}^{(4)}$$

Here:

$$
\begin{aligned}
f &= \alpha_2 J^{-4/3} \\
\frac{\partial f}{\partial \mathbf{C}} &= \alpha_2 \cdot \frac{d}{d\mathbf{C}}(J^{-4/3}) = -\frac{4}{3}\alpha_2 J^{-7/3} \cdot \frac{1}{2} J\mathbf{C}^{-1} = -\frac{2}{3}\alpha_2 J^{-4/3}\mathbf{C}^{-1}
\end{aligned}
$$

Therefore:

$$
\boxed{\frac{\partial f_2}{\partial \mathbf{C}} = -\frac{2}{3}\alpha_2 J^{-4/3}\mathbf{C}^{-1} \otimes \mathbf{C} + \alpha_2 J^{-4/3}\,\mathbb{I}^{(4)}} \tag{33}
$$

Derivative of f_3 with respect to C We define:

$$
f_3(\mathbf{C}) = -\frac{1}{3}\alpha_1 J^{-2/3} I_C - \frac{2}{3}\alpha_2 J^{-4/3} II_C + \frac{\alpha_3}{2} J(J-1) - \frac{1}{2}\beta(\theta - \theta_0)
$$

We split the expression into four terms:

$$
f_3 = f_{3A} + f_{3B} + f_{3C} + f_{3D}
$$

Term A: $f_{3A} = -\frac{1}{3}\alpha_1 J^{-2/3} I_C$

$$
\begin{aligned}
\frac{\partial f_{3A}}{\partial \mathbf{C}} &= -\frac{1}{3}\alpha_1 \left[\frac{d}{d\mathbf{C}}(J^{-2/3}) \cdot I_C + J^{-2/3} \cdot \frac{dI_C}{d\mathbf{C}}\right] \\
&= -\frac{1}{3}\alpha_1 \left[-\frac{1}{3} J^{-2/3} I_C \mathbf{C}^{-1} + J^{-2/3}\mathbf{I}\right] \\
&= \boxed{\frac{1}{9}\alpha_1 J^{-2/3} I_C \mathbf{C}^{-1} - \frac{1}{3}\alpha_1 J^{-2/3}\mathbf{I}}
\end{aligned} \tag{34}
$$

Term B: $f_{3B} = -\frac{2}{3}\alpha_2 J^{-4/3} II_C$

$$
\begin{aligned}
\frac{\partial f_{3B}}{\partial \mathbf{C}} &= -\frac{2}{3}\alpha_2 \left[\frac{d}{d\mathbf{C}}(J^{-4/3}) \cdot II_C + J^{-4/3} \cdot \frac{dII_C}{d\mathbf{C}}\right] \\
&= -\frac{2}{3}\alpha_2 \left[-\frac{2}{3} J^{-4/3} II_C \mathbf{C}^{-1} + J^{-4/3}(I_C\mathbf{I} - \mathbf{C})\right] \\
&= \boxed{\frac{4}{9}\alpha_2 J^{-4/3} II_C \mathbf{C}^{-1} - \frac{2}{3}\alpha_2 J^{-4/3}(I_C\mathbf{I} - \mathbf{C})}
\end{aligned} \tag{35}
$$

Term C: $f_{3C} = \frac{\alpha_3}{2} J(J-1)$

$$
\begin{aligned}
\frac{\partial f_{3C}}{\partial \mathbf{C}} &= \frac{\alpha_3}{2} \cdot \left[\frac{dJ}{d\mathbf{C}}(J-1) + J \cdot \frac{dJ}{d\mathbf{C}}\right] \\
&= \frac{\alpha_3}{2}(2J-1) \cdot \frac{1}{2} J\mathbf{C}^{-1} \\
&= \boxed{\frac{\alpha_3}{4} J(2J-1)\mathbf{C}^{-1}}
\end{aligned} \tag{36}
$$

Term D: $f_{3D} = -\frac{1}{2}\beta(\theta - \theta_0)$

$$
\boxed{\frac{\partial f_{3D}}{\partial \mathbf{C}} = \mathbf{0}} \tag{37}
$$

Combined Expression:

$$
\begin{aligned}
\frac{\partial f_3}{\partial \mathbf{C}} = &\frac{1}{9}\alpha_1 J^{-2/3} I_C \mathbf{C}^{-1} + \frac{4}{9}\alpha_2 J^{-4/3} II_C \mathbf{C}^{-1} + \frac{\alpha_3}{4} J(2J-1)\mathbf{C}^{-1} \\
&- \frac{1}{3}\alpha_1 J^{-2/3}\mathbf{I} - \frac{2}{3}\alpha_2 J^{-4/3}(I_C\mathbf{I} - \mathbf{C})
\end{aligned} \tag{38}
$$

Final Contribution to Tangent Tensor:

$$\boxed{\frac{\partial}{\partial \mathbf{C}}(f_3 \mathbf{C}^{-1}) = \left(\frac{\partial f_3}{\partial \mathbf{C}}\right) \otimes \mathbf{C}^{-1} - f_3 \cdot (\mathbf{C}^{-1} \otimes \mathbf{C}^{-1})} \tag{39}$$

Final Expression for Material Tangent Tensor $\frac{\partial \mathbf{S}}{\partial \mathbf{C}}$ We now combine all terms derived from f_1, f_2, and f_3 to construct the total fourth-order material tangent:

$$\boxed{\begin{aligned}\mathbb{C} = \frac{\partial \mathbf{S}}{\partial \mathbf{C}} = 2\Big[&\left(-\frac{1}{3}\alpha_1 J^{-2/3}\mathbf{C}^{-1} - \frac{2}{3}\alpha_2 J^{-4/3} I_C \mathbf{C}^{-1} + \alpha_2 J^{-4/3}\mathbf{I}\right) \otimes \mathbf{I} \\ &+ \left(-\frac{2}{3}\alpha_2 J^{-4/3}\mathbf{C}^{-1} \otimes \mathbf{C} + \alpha_2 J^{-4/3}\,\mathbb{I}^{(4)}\right) \\ &+ \left(\left[\frac{1}{9}\alpha_1 J^{-2/3} I_C \mathbf{C}^{-1} + \frac{4}{9}\alpha_2 J^{-4/3} II_C \mathbf{C}^{-1} + \frac{\alpha_3}{4} J(2J-1)\mathbf{C}^{-1} \right.\right. \\ &\left.\left. -\frac{1}{3}\alpha_1 J^{-2/3}\mathbf{I} - \frac{2}{3}\alpha_2 J^{-4/3}(I_C \mathbf{I} - \mathbf{C})\right] \otimes \mathbf{C}^{-1} - f_3 \cdot (\mathbf{C}^{-1} \otimes \mathbf{C}^{-1})\right)\Big]\end{aligned}} \tag{40}$$

where the scalar f_3 is:

$$f_3 = -\frac{1}{3}\alpha_1 J^{-2/3} I_C - \frac{2}{3}\alpha_2 J^{-4/3} II_C + \frac{\alpha_3}{2} J(J-1) - \frac{1}{2}\beta(\theta - \theta_0)$$

3.1.2 Derivative of S with respect to θ

The derivative of S with respect to θ is given by :

$$\frac{\partial \mathbf{S}}{\partial \theta} = 2\rho_o \left[-\frac{1}{2}\frac{\partial}{\partial \theta}\left(\beta(\theta - \theta_0))\right)\mathbf{C}^{-1}\right] \tag{41}$$

$$\boxed{\frac{\partial \mathbf{S}}{\partial \theta} = -\rho_o \beta \mathbf{C}^{-1}} \tag{42}$$

3.2 Simo and Pister Material Model

Helmholtz–Energy Function.

$$\rho_0\,\Psi = \frac{\lambda}{2}\big(\ln J\big)^2 + \mu\left[\ln J + \frac{I_C - 3}{2}\right] - \beta\,\ln(J)\,(\theta-\theta_0) - \rho_0 c_\varepsilon\left[\theta\ln\!\left(\frac{\theta}{\theta_0}\right) - \theta + \theta_0\right], \qquad J = \det\mathbf{F},\ \ I_C = \operatorname{tr}\mathbf{C}. \tag{43}$$

Second Piola–Kirchhoff stress.

$$\mathbf{S} = \mu(\mathbf{I} - \mathbf{C}^{-1}) + \lambda\,\ln(J)\,\mathbf{C}^{-1} - \beta\,(\theta - \theta_0)\,\mathbf{C}^{-1}. \tag{44}$$

Residuum — balance of linear momentum.

$$R_u(\mathbf{u}, \theta, v_u) = \int_{\Omega_0} \mathbf{S} : \delta\mathbf{E}\,dV \;-\; \int_{\partial\Omega_0} \bar{t}\cdot v_u\,dA = 0, \qquad \delta\mathbf{E}(\mathbf{u}, v_u) = \operatorname{sym}(\mathbf{F}^\top\nabla_x v_u). \tag{45}$$

Linearization of balance of linear momentum.

$$\mathrm{LIN}[R_u] = R_u(\tilde{\mathbf{u}}, \tilde{\theta}, v_u) + \int_{\Omega_0} \delta\tilde{\mathbf{E}} : \hat{\mathbb{C}} : \Delta\mathbf{C}\;dV + \int_{\Omega_0} \nabla_x(\Delta\mathbf{u}) : \tilde{\mathbf{S}} : \nabla_x(v_u)\;dV - \int_{\Omega_0} \beta\,\delta\tilde{\mathbf{E}} : \mathbf{C}^{-1}\,\Delta\theta\;dV. \tag{46}$$

with the following terms

$$\hat{\mathbb{C}}(\mathbf{u}, \theta) = \big(\lambda\ln J - \mu - \beta[\theta - \theta_0]\big)\,\frac{\partial\mathbf{C}^{-1}}{\partial\mathbf{C}} \;+\; \frac{\lambda}{2}\,\mathbf{C}^{-1}\otimes\mathbf{C}^{-1}, \tag{47}$$

$$\frac{\partial\mathbf{C}^{-1}}{\partial\mathbf{C}} = -\frac{1}{2}\Big(\big(\mathbf{C}^{-1}\otimes\mathbf{C}^{-1}\big)^{23\mathrm{T}} + \big(\mathbf{C}^{-1}\otimes\mathbf{C}^{-1}\big)^{24\mathrm{T}}\Big), \qquad \Delta\mathbf{C} = 2\,\operatorname{sym}\big(\mathbf{F}^\top\nabla_x(\Delta\mathbf{u})\big), \qquad \delta\tilde{\mathbf{E}} = \operatorname{sym}\big(\tilde{\mathbf{F}}^\top\nabla_x v_u\big). \tag{48}$$

3.3 Linearization of Energy Balance R_θ

The residual form of the energy balance in the reference configuration is given by:

$$R_\theta(\mathbf{u}, \theta, v_\theta) = \int_{\Omega_0} \rho_0 c_\varepsilon \dot{\theta}\, v_\theta \, dV + \int_{\Omega_0} \beta\theta \, \mathrm{Grad}(\dot{\mathbf{x}}) \cdot \mathbf{F}^{-T} \, v_\theta \, dV - \int_{\Omega_0} \mathbf{Q} \cdot \mathrm{Grad}(v_\theta) \, dV + \int_{\partial\Omega_0} \mathbf{Q} \cdot \mathbf{N} \, dA \quad (49)$$

Here:

- ρ_0 is the reference density,
- C_ε is the specific heat,
- θ is temperature,
- $\mathbf{Q} = -kJ\mathbf{C}^{-1}\mathrm{Grad}(\theta)$ is the heat flux vector in the reference configuration,
- $\mathbf{F}$ is the deformation gradient, and
- $\mathbf{C} = \mathbf{F}^T\mathbf{F}$ is the right Cauchy-Green deformation tensor.

The linearization of this residual around a trial solution $\theta = \theta^k$ is expressed as:

$$\begin{aligned} \mathrm{LIN}[R_\theta] = R_\theta(\mathbf{u}, \theta, v_\theta) + \int_{\Omega_u} \Big[\frac{\partial R_\theta}{\partial \theta}\Big|_{\tilde{\theta}} \cdot \Delta\theta + \frac{\partial R_\theta}{\partial \theta'}\Big|_{\tilde{\theta}} \cdot \Delta\theta' + \frac{\partial R_\theta}{\partial(\nabla \mathbf{x}(\theta))}\Big|_{\tilde{\theta}} \cdot \Delta(\nabla \mathbf{x}(\theta)) \\ + \frac{\partial R_\theta}{\partial(\nabla \mathbf{x}(\mathbf{x}'))}\Big|_{\tilde{\mathbf{u}}} \cdot \Delta(\nabla \mathbf{x}(\mathbf{x}')) + \frac{\partial R_\theta}{\partial \mathbf{C}}\Big|_{\tilde{\mathbf{u}}} \cdot \Delta\mathbf{C} + \frac{\partial R_\theta}{\partial \mathbf{F}}\Big|_{\tilde{\mathbf{u}}} \cdot \Delta\mathbf{F} \Big] \, dV \end{aligned} \quad (50)$$

To evaluate the tangent terms above, we now derive each contribution separately.

3.3.1 Derivative with respect to θ:

This term arises from the transient heat capacity term:

$$\frac{\partial R_\theta}{\partial \theta} \cdot \Delta\theta = v_\theta \, \beta \, \nabla_X \mathbf{x}(\mathbf{x}') \cdot \mathbf{F}^{-T} \, \Delta\theta \quad (51)$$

3.3.2 Derivative with respect to θ':

The dependence on θ' comes from the thermomechanical coupling term:

$$\frac{\partial R_\theta}{\partial \theta'} \cdot \Delta\theta' = v_\theta \, \rho_0 c_\varepsilon \, \frac{\Delta\theta}{\Delta t} \quad (52)$$

Auxiliary tensorial identities: These will be used later in the derivatives involving $\mathbf{C}$:

$$\frac{\partial J}{\partial C} = \frac{1}{2} J\mathbf{C}^{-1} \quad (53)$$

$$\frac{\partial(\mathbf{C}^{-1})}{\partial C} = -\mathbf{C}^{-1} \otimes \mathbf{C}^{-1} \quad (54)$$

3.3.3 Derivative of Residual R_θ with respect to $\nabla_X\theta$

From the weak form, keep only the conduction term that depends on $\nabla_X\theta$:

$$R_\theta^{\mathrm{cond}} = -\int_{\Omega_0} \mathbf{Q} \cdot \nabla_X v_\theta \, dV, \qquad \mathbf{Q} = -\,\kappa \, J \, \mathbf{C}^{-1} \, \nabla_X\theta. \quad (55)$$

Since $\partial\mathbf{Q}/\partial(\nabla_X\theta) = -\,\kappa\, J\, \mathbf{C}^{-1}$, the Gâteaux derivative of R_θ^{cond} in the direction $\nabla_X(\Delta\theta)$ is

$$\begin{aligned} \frac{\partial R_\theta}{\partial(\nabla_X\theta)} \; : \; \nabla_X(\Delta\theta) &= -\int_{\Omega_0} \left(\frac{\partial \mathbf{Q}}{\partial(\nabla_X\theta)} \, \nabla_X(\Delta\theta) \right) \cdot \nabla_X v_\theta \, dV \\ &= \int_{\Omega_0} \nabla_X v_\theta \; \cdot \; \kappa \, J \, \mathbf{C}^{-1} \; \cdot \; \nabla_X(\Delta\theta) \, dV. \end{aligned} \quad (56)$$

Equivalently, the pointwise integrand relation (matching the screenshot) is

$$\frac{\partial R_\theta}{\partial(\nabla_X\theta)} \cdot \nabla_X(\Delta\theta) = \nabla_X v_\theta \cdot \kappa \, J \, \mathbf{C}^{-1} \cdot \nabla_X(\Delta\theta) \quad (57)$$

3.3.4 Derivative of Residual R_θ with respect to $\mathbf{C}$

Consider only the conduction contribution (the part depending on $\mathbf{C}$):

$$R_\theta^{\text{cond}} \;=\; \int_{\Omega_0} \kappa\, J\, \mathbf{C}^{-1} : \left(\nabla_X \theta \otimes \nabla_X v_\theta\right) dV, \qquad \mathbf{Q} = -\kappa J \mathbf{C}^{-1} \nabla_X \theta.$$

For a variation $\Delta\mathbf{C}$, use

$$\Delta J = \tfrac{1}{2}\, J\, \mathbf{C}^{-1} : \Delta\mathbf{C}, \qquad \Delta(\mathbf{C}^{-1}) = -\,\mathbf{C}^{-1}\,(\Delta\mathbf{C})\,\mathbf{C}^{-1}.$$

Then

$$\Delta\Big(J\mathbf{C}^{-1}\Big) = \tfrac{1}{2}\, J\,(\mathbf{C}^{-1} : \Delta\mathbf{C})\,\mathbf{C}^{-1} \;-\; J\,\mathbf{C}^{-1}(\Delta\mathbf{C})\mathbf{C}^{-1}.$$

Writing the result with standard fourth-order tensor notation, the pointwise (integrand) directional derivative is

$$\begin{aligned}\frac{\partial R_\theta}{\partial \mathbf{C}} : \Delta\mathbf{C} &= \kappa\,\frac{J}{2}\,(\mathbf{C}^{-1}\otimes\mathbf{C}^{-1}) : (\nabla_X\theta \otimes \nabla_X v_\theta) : \Delta\mathbf{C} \\ &\quad - \kappa\,\frac{J}{2}\Big((\mathbf{C}^{-1}\otimes\mathbf{C}^{-1})^{23\mathrm{T}} + (\mathbf{C}^{-1}\otimes\mathbf{C}^{-1})^{24\mathrm{T}}\Big) : (\nabla_X\theta \otimes \nabla_X v_\theta) : \Delta\mathbf{C}.\end{aligned} \tag{58}$$

Equivalently, in the compact "dot" style matching the screenshot:

$$\frac{\partial R_\theta}{\partial \mathbf{C}} \cdot \Delta\mathbf{C} = \kappa\,\frac{J}{2}\,(\mathbf{C}^{-1}\otimes\mathbf{C}^{-1}) \cdot \nabla_X\theta \cdot \nabla_X v_\theta \cdot \Delta\mathbf{C} - \kappa\,\frac{J}{2}\Big((\mathbf{C}^{-1}\otimes\mathbf{C}^{-1})^{23\mathrm{T}} + (\mathbf{C}^{-1}\otimes\mathbf{C}^{-1})^{24\mathrm{T}}\Big) \cdot \nabla_X\theta \cdot \nabla_X v_\theta \cdot \Delta\mathbf{C} \tag{59}$$

3.3.5 Derivative of Residual R_θ with respect to $\mathbf{F}$

Starting from the thermal residual in the reference configuration,

$$R_\theta(\mathbf{u},\theta,v_\theta) = \int_{\Omega_0} \rho_0 C_\varepsilon\, \dot\theta\, v_\theta\, dV - \int_{\Omega_0} \mathbf{Q}\cdot\nabla_X v_\theta\, dV + \int_{\Omega_0} \beta\theta\,\nabla_X(\dot{\mathbf{x}}) : \mathbf{F}^{-T}\, v_\theta\, dV,$$

only the *coupling* term depends explicitly on $\mathbf{F}$. Denote

$$\mathcal{C} \;:=\; \beta\theta\,\nabla_X(\dot{\mathbf{x}}) : \mathbf{F}^{-T}\, v_\theta.$$

For a variation $\Delta\mathbf{F}$, use the standard identity

$$\Delta(\mathbf{F}^{-T}) = -\,\mathbf{F}^{-T}\,(\Delta\mathbf{F})^T\,\mathbf{F}^{-T}.$$

Writing the double contraction with a fourth-order mapping,

$$\nabla_X(\dot{\mathbf{x}}) : \Delta(\mathbf{F}^{-T}) = -\Big[\big(\mathbf{F}^{-T}\otimes\mathbf{F}^{-T}\big)^{24\mathrm{T}} : \nabla_X(\dot{\mathbf{x}})\Big] : \Delta\mathbf{F},$$

so that the Gâteaux derivative of the coupling integrand w.r.t. $\mathbf{F}$ in the direction $\Delta\mathbf{F}$ is

$$\frac{\partial\mathcal{C}}{\partial\mathbf{F}} : \Delta\mathbf{F} = -\,v_\theta\,\beta\,\theta\,\Big[\big(\mathbf{F}^{-T}\otimes\mathbf{F}^{-T}\big)^{24\mathrm{T}} : \nabla_X(\dot{\mathbf{x}})\Big] : \Delta\mathbf{F}.$$

Using $\nabla_X(\dot{\mathbf{x}}) = \nabla_X(\mathbf{x}')$ with $\mathbf{x}'$ the material time derivative of the displacement map, the pointwise (integrand) relation becomes

$$\boxed{\frac{\partial R_\theta}{\partial\mathbf{F}}\cdot\Delta\mathbf{F} = -\,v_\theta\,\beta\,\theta\,\nabla_X(\mathbf{x}')\cdot\big(\mathbf{F}^{-T}\otimes\mathbf{F}^{-T}\big)^{24\mathrm{T}}\cdot\nabla_X(\Delta\mathbf{u})} \tag{60}$$

which matches the structure shown in the figure (no boundary terms, integrand form).

Approximating time derivatives. For a first-order implicit (backward Euler) approximation,

$$\mathbf{x}' \;=\; \frac{\mathbf{u}-\mathbf{u}^n}{\Delta t} \qquad\text{and}\qquad \theta' \;=\; \frac{\theta-\theta^n}{\Delta t} \tag{61}$$

so that $\nabla_X(\mathbf{x}') = \dfrac{\nabla_X(\Delta\mathbf{u})}{\Delta t}$ if the gradient operator and time increment commute under the chosen discretization.

3.3.6 Fully Assembled Tangent Operator for R_θ

$$\begin{aligned}
\mathrm{Lin}[R_\theta] &= R_\theta(\tilde{\mathbf{u}},\tilde\theta,v_\theta)\\
&\quad + \int_{\Omega_0}\Big\{v_\theta\,\rho_0 c_\varepsilon\,\frac{\Delta\theta}{\Delta t} + v_\theta\,\beta\,\nabla_X\mathbf{x}(\mathbf{x}')\cdot\mathbf{F}^{-T}\,\Delta\theta + \nabla_X v_\theta\cdot\kappa J\mathbf{C}^{-1}\cdot\nabla_X(\Delta\theta)\Big\}\,dV\\
&\quad + \int_{\Omega_0} v_\theta\,\beta\theta\,\mathbf{F}^{-T}\cdot\frac{\nabla_X(\Delta\mathbf{u})}{\Delta t}\,dV\\
&\quad + \int_{\Omega_0}\Big[\kappa\frac{J}{2}\,(\mathbf{C}^{-1}\otimes\mathbf{C}^{-1}) - \kappa\frac{J}{2}\Big((\mathbf{C}^{-1}\otimes\mathbf{C}^{-1})^{23\mathrm{T}} + (\mathbf{C}^{-1}\otimes\mathbf{C}^{-1})^{24\mathrm{T}}\Big)\Big] : (\nabla_X\theta\otimes\nabla_X v_\theta) : \Delta\mathbf{C}\,dV\\
&\quad + \int_{\Omega_0}\Big(-\,v_\theta\,\beta\,\theta\Big)\Big[(\mathbf{F}^{-T}\otimes\mathbf{F}^{-T})^{24\mathrm{T}} : \nabla_X(\mathbf{x}')\Big] : \Delta\mathbf{F}\,dV
\end{aligned} \tag{62}$$

4 Discretization

4.1 Space Discretization

We discretize our field quantities and test functions using shape functions as follows:

$$
\begin{aligned}
u &= \sum_I \phi^I d_u^I, & \delta u &= \sum_I \phi^I \delta d_u^I, & \Delta u &= \sum_I \phi^I \Delta d_u^I, \\
C &= \sum_I 2B_I^u d_u^I, & \delta E &= \sum_I B_I^u \delta d_u^I, & \Delta C &= \sum_I 2B_I^u \Delta d_u^I, \\
\theta &= \sum_I \phi^I d_\theta^I, & \delta\theta &= \sum_I \phi^I \delta d_\theta^I, & \Delta\theta &= \sum_I \phi^I \Delta d_\theta^I, \\
\nabla\theta &= \sum_I L_I d_\theta^I, & \delta\nabla\theta &= \sum_I L_I \delta d_\theta^I, & \Delta\nabla\theta &= \sum_I L_I \Delta d_\theta^I.
\end{aligned}
$$

- u is the element displacement
- ϕ is the shape function
- d_u is the nodal displacement
- δd_u is the virtual nodal displacement
- Δd_u is the incremental nodal displacement
- B is the discrete Grad operator
- θ is the element temperature
- d_θ is the nodal temperature
- δd_θ is the virtual nodal temperature
- Δd_θ is the incremental nodal temperature
- L is the shape function derivative

Using shape functions and writing the equation in matrix notation, we get:

$$
B_{NL}^u = \begin{bmatrix} \hat{F}_{11}\phi_{,1}^I & \hat{F}_{21}\phi_{,1}^I \\ \hat{F}_{12}\phi_{,2}^I & \hat{F}_{22}\phi_{,2}^I \\ \hat{F}_{11}\phi_{,2}^I + \hat{F}_{12}\phi_{,1}^I & \hat{F}_{21}\phi_{,2}^I + \hat{F}_{22}\phi_{,1}^I \end{bmatrix}, \qquad L^I = \begin{bmatrix} \phi_{,1}^I \\ \phi_{,2}^I \end{bmatrix}.
$$

where,

$$
[S]^V = \begin{bmatrix} S_{11} \\ S_{22} \\ S_{12} \end{bmatrix}, \quad \left[\frac{\partial S}{\partial C}\right]^V = \begin{bmatrix} C_{1111} & C_{1122} & C_{1112} \\ C_{2211} & C_{2222} & C_{2212} \\ C_{1211} & C_{1222} & C_{1212} \end{bmatrix}.
$$

4.2 Time Discretization

The Backward Euler time discretization approximates the time derivatives as:

$$\dot{\theta}_{n+1} = \frac{\theta_{n+1} - \theta_n}{\Delta t}, \qquad \frac{\partial \dot{\theta}_{n+1}}{\partial \theta_{n+1}} = \frac{1}{\Delta t},$$

$$\Delta\dot{\theta}_{n+1} = \frac{\Delta\theta_{n+1}}{\Delta t}, \qquad \Delta\dot{u}_{n+1} = \frac{\Delta u_{n+1}}{\Delta t}.$$

These equations are implicit and typically require solving a nonlinear system at each time step. The discretized coupled system at time t_{n+1} with Backward Euler time integration:

$$\begin{bmatrix} \mathbf{K}_{uu,n+1} & \mathbf{K}_{u\theta,n+1} \\ \mathbf{K}_{\theta u,n+1} & \mathbf{K}_{\theta\theta,n+1} \end{bmatrix} \begin{bmatrix} \Delta\mathbf{du}_{n+1} \\ \Delta\mathbf{d}\theta_{n+1} \end{bmatrix} = -\begin{bmatrix} \mathbf{R}_{u,n+1} \\ \mathbf{R}_{\theta,n+1} \end{bmatrix} \tag{63}$$

where all quantities are evaluated at t_{n+1} and the time derivatives are approximated using:

$$\dot{\mathbf{u}}_{n+1} = \frac{\mathbf{u}_{n+1} - \mathbf{u}_n}{\Delta t} = \frac{\Delta\mathbf{u}_{n+1}}{\Delta t} \tag{64}$$

$$\dot{\theta}_{n+1} = \frac{\theta_{n+1} - \theta_n}{\Delta t} = \frac{\Delta\theta_{n+1}}{\Delta t} \tag{65}$$

The Backward Euler method provides first-order accuracy and unconditional stability for the time integration of the coupled thermo-mechanical system.

4.3 Discretized Weak Form

$$\begin{bmatrix}\delta u & \delta\theta\end{bmatrix}\begin{bmatrix}K_{uu} & K_{u\theta}\\ K_{\theta u} & K_{\theta\theta}\end{bmatrix}\begin{Bmatrix}\Delta u\\ \Delta\theta\end{Bmatrix} = -\begin{Bmatrix}R_u\\ R_\theta\end{Bmatrix}$$

With the above results, the discretized, linearized weak forms are given by:

$$\mathrm{LIN}[R_u] = R_u(\tilde{\mathbf{u}}, \tilde{\theta}, v_u) + \sum_N \alpha_n \det J_e \sum_I \sum_J \delta\mathbf{d}u_i^\mathsf{T}\, (B^I_{NL})^\mathsf{T} \left[\frac{\partial S}{\partial C}\right]^V (2B^J_{NL}\, \Delta\mathbf{d}u_j) \tag{66}$$

$$+ \sum_N \alpha_n \det J_e \sum_I \sum_J \delta\mathbf{d}u_i^\mathsf{T}\, (L^I)^\mathsf{T}\, \hat{S}\, L^J\, \Delta\mathbf{d}u_j \tag{67}$$

$$- \sum_N \alpha_n \det J_e \sum_I \sum_J \delta\mathbf{d}u_i^\mathsf{T}\, (B^I_{NL})^\mathsf{T}\, \frac{\partial S}{\partial\theta}\, \phi^J\, \Delta\mathbf{d}\theta^J. \tag{68}$$

In matrix form:

$$\mathrm{LIN}[R_u] = R_u + \delta\mathbf{du}^\mathsf{T}\, [\,\mathbf{K}_{uu}\, \Delta\mathbf{du} + \mathbf{K}_{u\theta}\, \Delta\mathbf{d}\theta] = 0. \tag{69}$$

where the stiffness matrices are:

$$\mathbf{K}^{IJ}_{uu} = \sum_N \alpha_n \det J_e \left[(B^I_{NL})^\mathsf{T}\, \mathbb{C}^V\, (2B^J_{NL}) + (L^I)^\mathsf{T}\, S\, L^J\right], \tag{70}$$

$$\mathbf{K}^{IJ}_{u\theta} = -\sum_N \alpha_n \det J_e \left[(B^I_{NL})^\mathsf{T}\, (\beta\, C^{-1})^V\, \phi^J\right]. \tag{71}$$

$$R_u = R(\tilde{\mathbf{u}}, \theta, v_u) = -\sum_N \alpha_n \det J_e\, (B^I_{NL})^\mathsf{T}\, [S]^V. \tag{72}$$

$$\mathrm{LIN}[R_\theta] = R_\theta(\mathbf{u}, \tilde{\theta}, v_\theta) \tag{73}$$

$$+ \sum_N \alpha_n \det J_e \sum_I \sum_J \delta d\theta_i \left[\phi^I N_i \beta \nabla_X(\mathbf{x}') \cdot \mathbf{F}^{-T} \phi^J \Delta d\theta_j\right] \tag{74}$$

$$+ \sum_N \alpha_n \det J_e \sum_I \sum_J \delta d\theta_i \left[\phi^I N_i \rho_0 c_\varepsilon \frac{\phi^J \Delta d\theta_j}{\Delta t}\right] \tag{75}$$

$$+ \sum_N \alpha_n \det J_e \sum_I \sum_J \delta d\theta_i \left[(L^I_\theta)^T \cdot \kappa J \mathbf{C}^{-1} \cdot L^J_\theta \Delta d\theta_j\right] \tag{76}$$

$$+ \sum_N \alpha_n \det J_e \sum_I \sum_J \delta d\theta_i \left[\phi^I N_i \beta\theta \mathbf{F}^{-T} \cdot \frac{B^J_u \Delta du_j}{\Delta t}\right] \tag{77}$$

$$+ \sum_N \alpha_n \det J_e \sum_I \sum_J \delta d\theta_i \left[\phi^I \kappa \frac{J}{2} \left(\mathbf{C}^{-1} \otimes \mathbf{C}^{-1}\right) \cdot (L^J_\theta) \cdot (L^I_\theta) \cdot 2B^J_u \Delta du_j\right] \tag{78}$$

$$- \sum_N \alpha_n \det J_e \sum_I \sum_J \delta d\theta_i \left[\phi^I \kappa \frac{J}{2} \left((\mathbf{C}^{-1} \otimes \mathbf{C}^{-1})^{\frac{23}{T}} + (\mathbf{C}^{-1} \otimes \mathbf{C}^{-1})^{\frac{24}{T}}\right) \cdot (L^J_\theta) \cdot (L^I_\theta) \cdot 2B^J_u \Delta du_j\right] \tag{79}$$

$$- \sum_N \alpha_n \det J_e \sum_I \sum_J \delta d\theta_i \left[\phi^I N_i \beta\theta \nabla_X(\mathbf{x}') \cdot (\mathbf{F}^{-T} \otimes \mathbf{F}^{-T})^{\frac{24}{T}} \cdot B^J_u \Delta du_j\right] \tag{80}$$

In matrix form:

$$\text{LIN}[R_\theta] = R_\theta + \delta\mathbf{d}\theta^T \left[\mathbf{K}_{\theta u}\Delta\mathbf{d}\theta + \mathbf{K}_{\theta\theta}\Delta\mathbf{du}\right] = 0 \tag{81}$$

where the stiffness matrices are:

$$\mathbf{K}_{\theta u}^{IJ} = \sum_N \alpha_n \det J_e \left[\phi^I v_\theta \beta\theta \mathbf{F}^{-T} \cdot \frac{B_u^J}{\Delta t} + \phi^I \kappa \frac{J}{2} \mathbf{C}_{\text{deriv}} \cdot (L_\theta^J) \cdot (L_\theta^I) \cdot 2B_u^J \right. \tag{82}$$

$$\left. -\phi^I v_\theta \beta\theta \nabla_X(\mathbf{x}') \cdot (\mathbf{F}^{-T} \otimes \mathbf{F}^{-T})^{\frac{24}{T}} \cdot B_u^J \right] \tag{83}$$

$$\mathbf{K}_{\theta\theta}^{IJ} = \sum_N \alpha_n \det J_e \left[\phi^I v_\theta \beta \nabla_X(\mathbf{x}') \cdot \mathbf{F}^{-T} \phi^J + \phi^I v_\theta \rho_0 c_\varepsilon \frac{\phi^J}{\Delta t} + L_\theta^I \cdot \kappa J \mathbf{C}^{-1} \cdot L_\theta^J \right] \tag{84}$$

$$\tag{85}$$

where:

$$\mathbf{C}_{\text{deriv}} = \left(\mathbf{C}^{-1} \otimes \mathbf{C}^{-1}\right) - \left((\mathbf{C}^{-1} \otimes \mathbf{C}^{-1})^{\frac{23}{T}} + (\mathbf{C}^{-1} \otimes \mathbf{C}^{-1})^{\frac{24}{T}}\right) \tag{86}$$

$$\nabla_X(x') \cdot F^{-T} \nabla_v \theta = \frac{\dot{J}}{J} = \frac{1}{2}(\mathbf{C}^{-1} : \dot{\mathbf{C}}) \tag{87}$$

$$R_\theta(\mathbf{u}, \theta, v_\theta) = \sum_N \alpha_n \det J_e \sum_I \rho_0 c_\epsilon \dot{\theta} N_I \tag{88}$$

$$+ \sum_N \alpha_n \det J_e \sum_I \frac{\beta}{2} N_I \left(\mathbf{C}^{-1} : \dot{\mathbf{C}}\right) \theta_I \tag{89}$$

$$+ \sum_N \alpha_n \det J_e \sum_I kJ(L_\theta^I)^T \mathbf{C}^{-1} L^I \tag{90}$$

5 Results

5.1 Cantilever Beam

Geometry – ($1.5\,\mathrm{m} \times 0.1\,\mathrm{m} \times 0.1\,\mathrm{m}$) beam
Boundary Conditions –

I. *Dirichlet boundary conditions*
At $x = 0$, $\mathbf{u} = \mathbf{0}$

II. *Neumann boundary conditions*
At $x = L$, $\mathbf{t} = \{(0,\, 10000)\}\,\mathrm{kN/m^2}$

Following results are obtained on a mesh of $120 \times 8 \times 2$ second-order triangular elements.

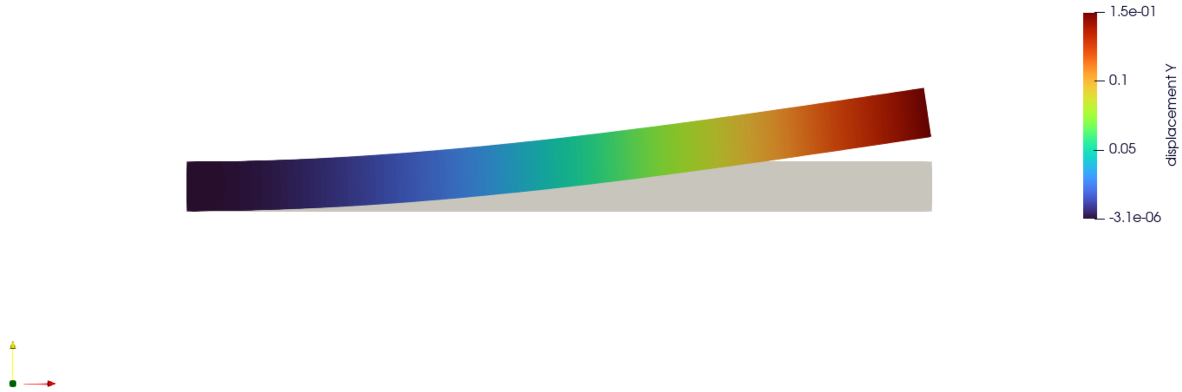

Figure 1: Displacement plot for non-linear case at maximum force

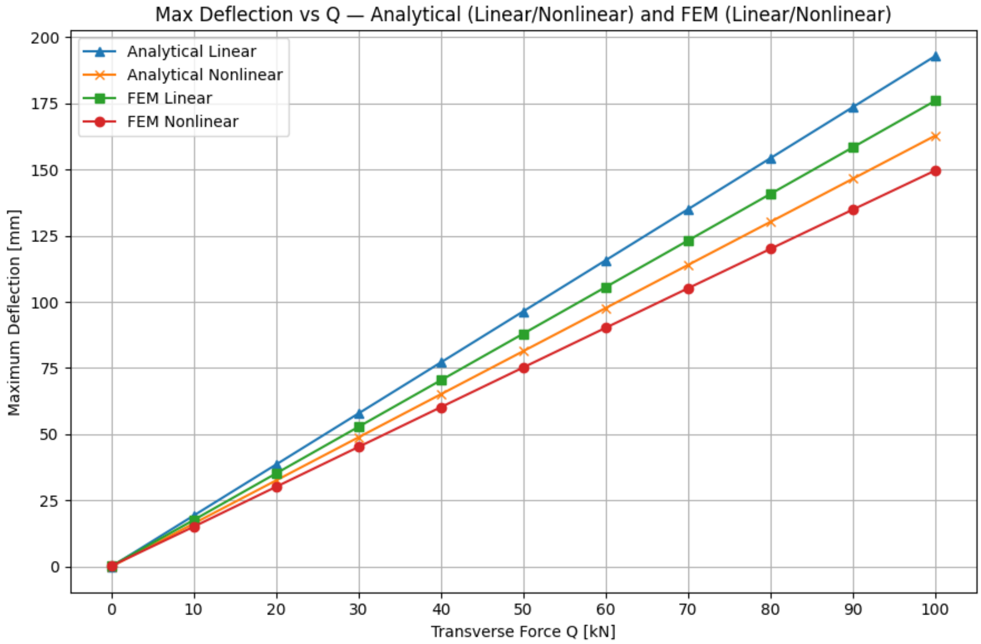

Figure 2: Max Deflection vs Q — Analytical (Linear/Nonlinear) and FEM (Linear/Nonlinear).

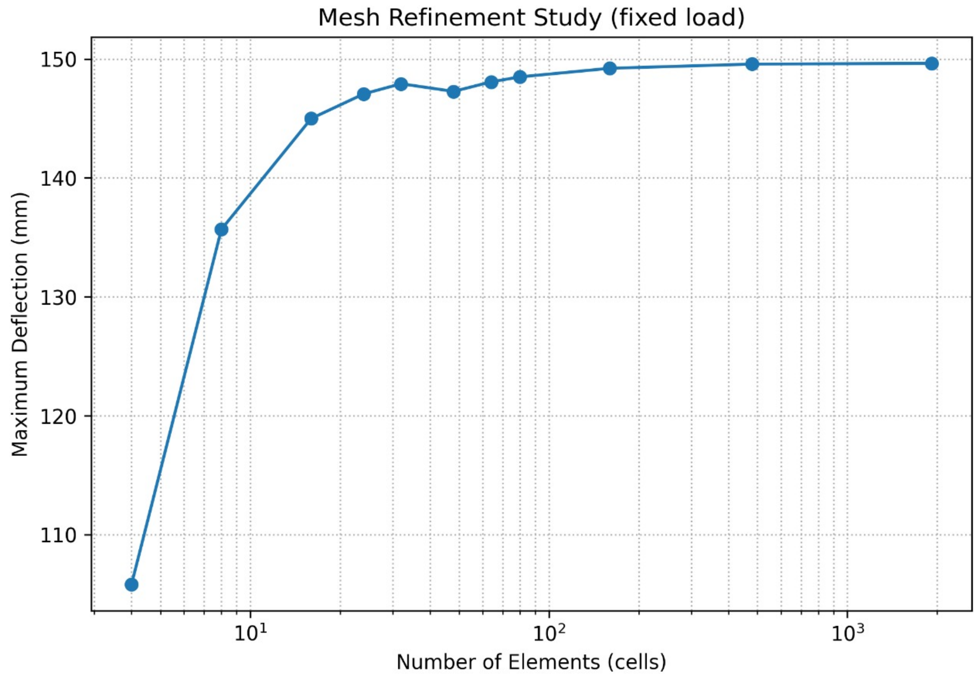

Figure 3: Mesh refinement study (maximum deflection vs. number of elements)

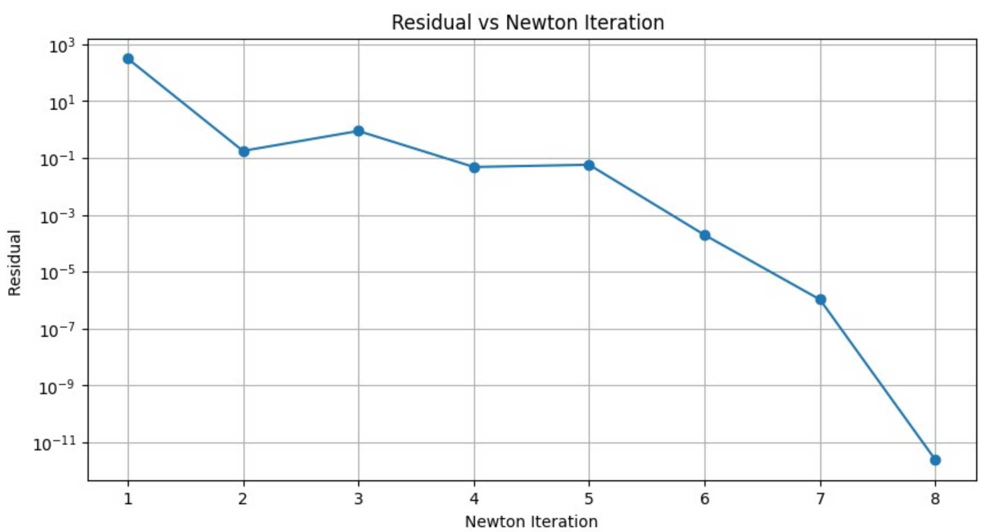

Figure 4: Newton iteration convergence graph

Load	**Newton iterations required for convergence**	**Deflection (mm)**
0	3	000.000
10	5	015.85
20	6	030.148
30	6	045.200
40	6	060.232
50	6	075.238
60	6	090.211
70	6	105.144
80	7	120.030
90	7	134.862
100	8	149.634

Fig. 4. Newton iteration and displacements obtained for the direct change in transverse force.

Load	**Newton iterations required for convergence**	**Deflection (mm)**
0	3	000.000
10	4	015.059
20	4	030.117
30	4	045.169
40	4	060.206
50	4	075.219
60	4	090.199
70	4	105.138
80	4	120.029
90	4	134.862
100	4	149.629

Fig. 5. Newton iterations required for convergence under gradual transverse-load increments.

5.2 Bimetallic Strip

Geometry – ($100\,\mathrm{mm} \times 1.5\,\mathrm{mm} \times 1\,\mathrm{mm}$) strip
Domains – Domain 1: > 0.6; Domain 2: < 0.6
Initial condition – At t=0, $T = 300\,\mathrm{K} =: T_0$
Boundary Conditions –

I. *Dirichlet boundary conditions*
(a) At x=0, $\mathbf{u} = \mathbf{0}$; (b) At x=0, $T = T_0$

II. *Neumann boundary conditions*
(a) At y=0, y=L, x=L, $q = 350\ \mathrm{mJ/(s \cdot mm^2)}$

Following results are obtained on a mesh of $60 \times 05 \times 2$ second-order triangular elements.

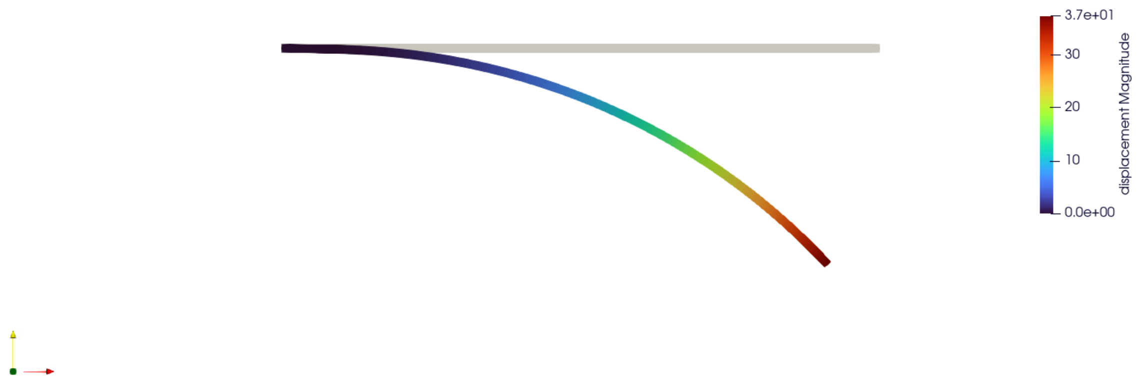

Figure 5: Plot for maximum deflection (I)

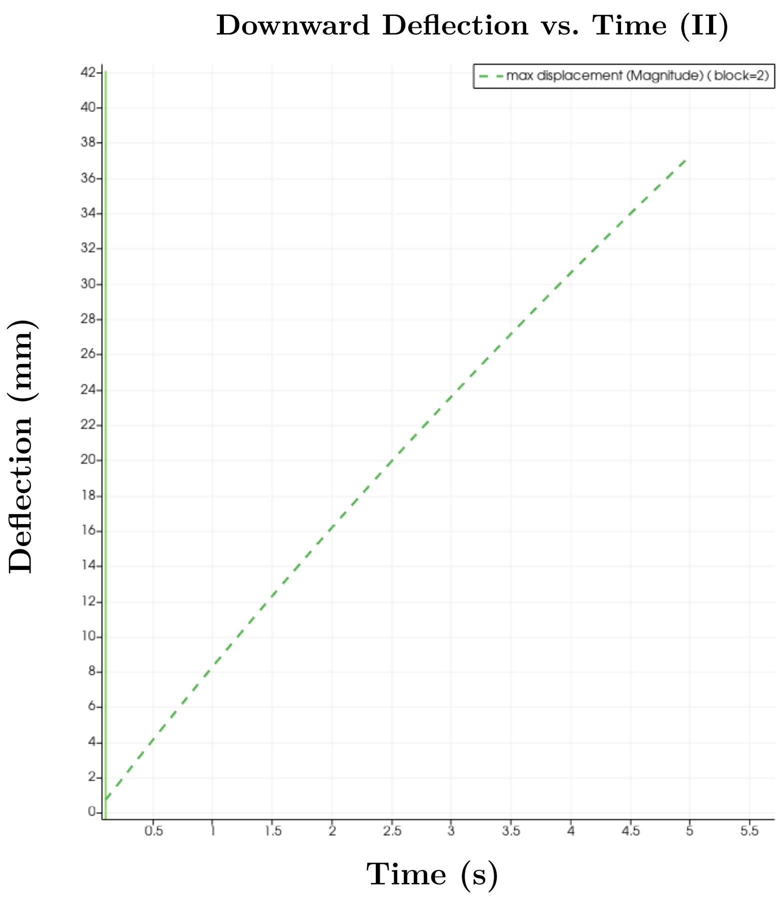

Figure 6: Downward deflection vs. time (II)

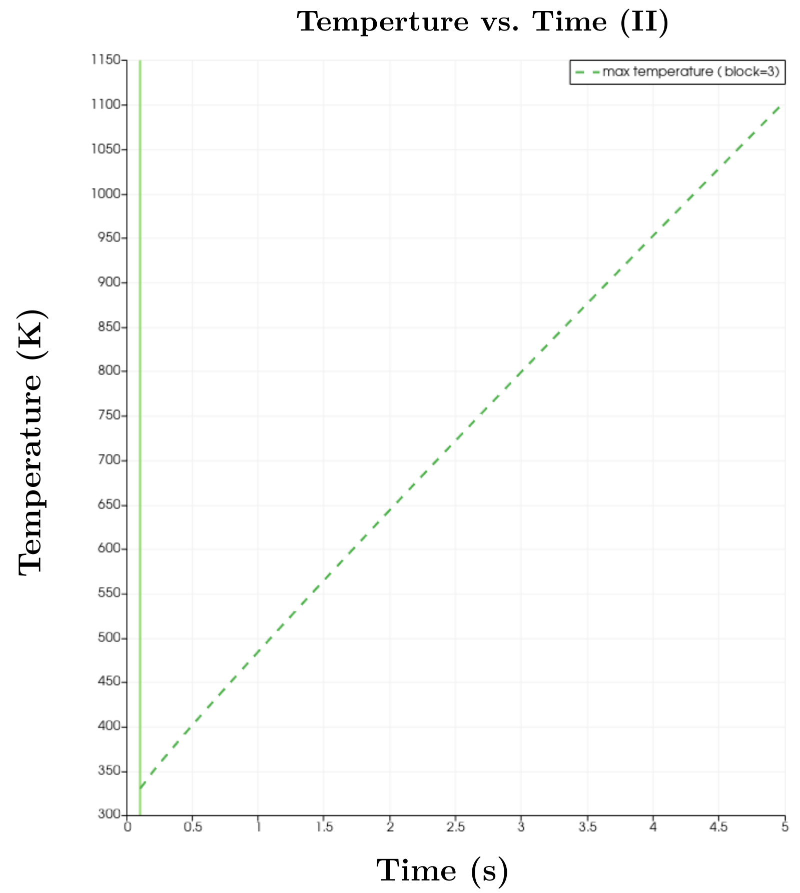

Figure 7: Temperature vs. time (II)

Figure 8: Plot for maximum temperature (II)

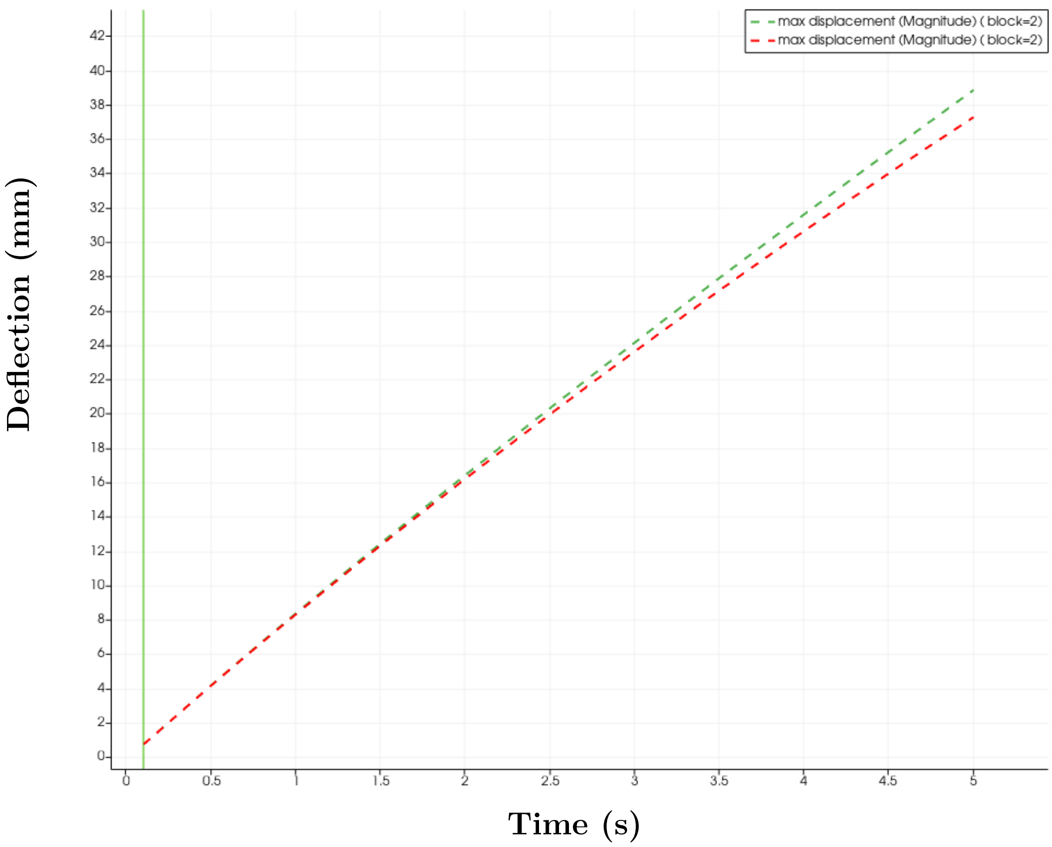

Figure 9: Comparison of Deflection for nonlinear and linear code.

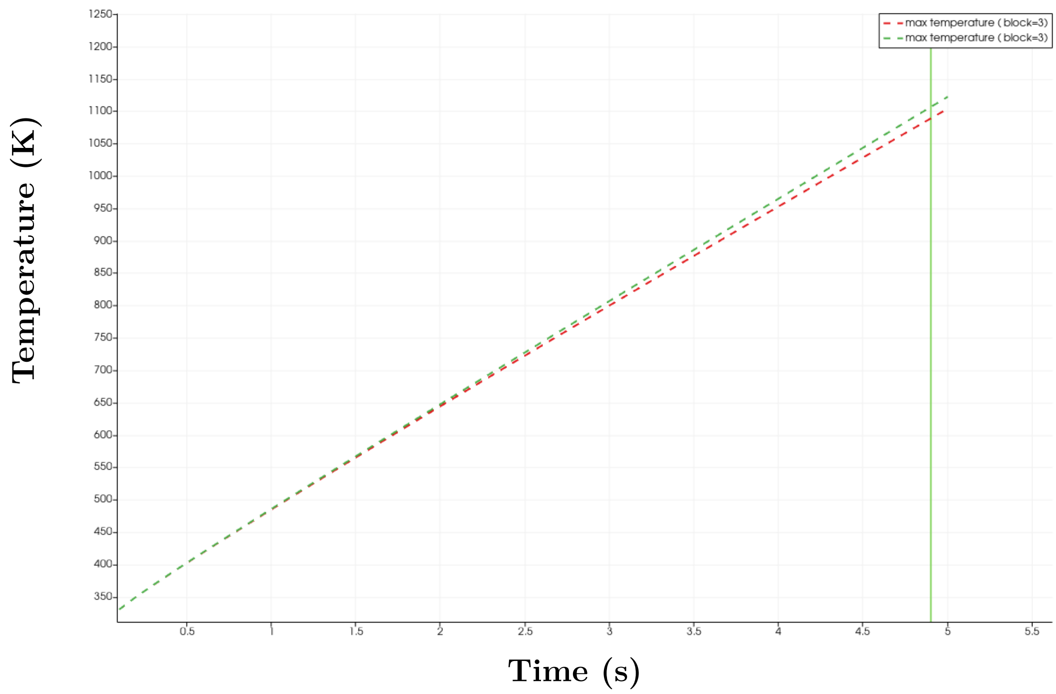

Figure 10: Comparison of Temperature for nonlinear and linear code.

Determination of Switch Disconnect from the Bimetallic Strip. The disconnect time is the instant when the mid-span displacement reaches 5 mm. The plot below depicts the deformed shape at $t = 0.6\,\mathrm{s}$ at the instant of disconnect.

Figure 11: Switch disconnect deformed shape

5.3 Conclusions for Part I (Cantilever Beam)

Following results are obtained on a mesh of $120 \times 8 \times 2$ second-order triangular elements.

1. Switching to the non-linear equations for the cantilever beam causes stiffening and shows lower tip deflections than the linear case.

2. Increasing the load increases the tip deflections approximately linearly.

3. Refining the mesh beyond 120 ($12 \times 8 \times 2$) elements changes only the 4th significant digit of the tip deflection.

4. The number of Newton iterations required for convergence with increasing loads is non-uniform.

5. Applying the full load in a single step required about **8** Newton iterations to converge, whereas using gradual load increments required only **3–4** iterations per increment. This is expected: with incremental loading the predictor for step m is the converged solution from the previous step ($\mathbf{u}_{(m)}^{k=0} = \mathbf{u}_{(m-1)}^{\star}$), so the initial residual is small and quadratic convergence is reached quickly. In contrast, a single large load step starts far from the new equilibrium, so the predictor is poor and more iterations are needed.

Table 1: Comparison of FEM and analytical solutions (tip deflection in mm)

Case	FEM Solution	Analytical Solution
Linear	175.971	192.857
Non-Linear	149.634	162.783

5.4 Conclusions for Part II (Bimetallic Strip)

1. Switching to a non-linear model increases the system's stiffness. As a result, the structure resists deformation more effectively. Consequently, non-linear analyses predict smaller deflections compared to linear solutions.

2. The switch disconnect time remains approximately the same for both linear and nonlinear models under this load. Nonlinear effects, however, become more significant at later times.(see comparison plots in Figure 09 and Figure 10).

3. The results show that finer meshes and higher-order elements provide slightly more accurate predictions of temperature and deflection, while coarser meshes and lower-order elements introduce minor deviations. Overall, non-linear models predict lower deflections and temperatures compared to linear models, highlighting the effect of nonlinearity.

Table 2: Mesh study for bimetallic strip

Case	Max Temperature (K)	Max Deflection (mm)
NonLinear 2^{nd} order, fine mesh	1093.1	-36.365
NonLinear 2^{nd} order, coarse mesh 60×5	1103.969	36.3645
NonLinear 1^{st} order, fine mesh 120×20	1102.99	35.8798
NonLinear 1^{st} order, coarse mesh 40×5	1104.10	37.7051
Linear 2^{nd} order, fine 120×20	1122.89	38.8354
Linear 2^{nd} order, coarse 60×5	1122.38	38.8343

4. For 2^{nd}-order elements, results on a coarse mesh are almost identical to those on a fine mesh.

5. 1^{st}order elements produce comparable results on a fine mesh; on a coarse mesh, deviation is observed.

6 References

1. Lecture Notes, Simulation of Coupled Problems, SoSe2025, University of Stuttgart.
2. Nonlinear Solid Mechanics: A Continuum Approach for Engineering, G. Holzapfel.
3. Nonlinear Finite Element Method, Peter Wriggers.

7 Appendix

7.1 Newton iterations per time step — Exam Task (linear cantilever case)

Table 3: Newton iterations and residuals at each load step.

Load ($\times 10^5$ N)	Newton iter	Residual
0.0	1	1.65×10^{2}
0.0	2	6.04×10^{-13}
10.0	1	2.83×10^{-1}
10.0	2	7.43×10^{-11}
20.0	1	2.83×10^{-1}
20.0	2	7.43×10^{-11}
30.0	1	2.83×10^{-1}
30.0	2	7.43×10^{-11}
40.0	1	2.83×10^{-1}
40.0	2	7.43×10^{-11}
50.0	1	2.83×10^{-1}
50.0	2	7.43×10^{-11}
60.0	1	2.83×10^{-1}
60.0	2	7.43×10^{-11}
70.0	1	2.83×10^{-1}
70.0	2	7.43×10^{-11}
80.0	1	2.83×10^{-1}
80.0	2	7.43×10^{-11}
90.0	1	2.83×10^{-1}
90.0	2	7.43×10^{-11}
100.0	1	2.83×10^{-1}
100.0	2	7.43×10^{-11}

7.2 Newton iterations per time step — Exam Task (nonlinear cantilever case)

Table 4: Newton iterations and residuals at each load step.

Load ($\times 10^5$ N)	Newton iter	Residual
0.0	1	3.20×10^{2}
0.0	2	9.85×10^{-6}
0.0	3	6.82×10^{-10}
10.0	1	4.71×10^{-1}
10.0	2	2.54×10^{-3}
10.0	3	1.56×10^{-5}
10.0	4	1.63×10^{-9}
20.0	1	4.71×10^{-1}
20.0	2	2.54×10^{-3}
20.0	3	2.76×10^{-5}
20.0	4	2.21×10^{-9}
30.0	1	4.70×10^{-1}
30.0	2	2.54×10^{-3}
30.0	3	4.68×10^{-5}
30.0	4	3.40×10^{-9}
40.0	1	4.70×10^{-1}
40.0	2	2.54×10^{-3}
40.0	3	6.70×10^{-5}
40.0	4	4.74×10^{-9}
50.0	1	4.69×10^{-1}
50.0	2	2.54×10^{-3}
50.0	3	8.72×10^{-5}
50.0	4	6.11×10^{-9}
60.0	1	4.68×10^{-1}
60.0	2	2.54×10^{-3}
60.0	3	1.07×10^{-4}
60.0	4	7.46×10^{-9}
70.0	1	4.67×10^{-1}
70.0	2	2.55×10^{-3}
70.0	3	1.26×10^{-4}
70.0	4	8.77×10^{-9}
80.0	1	4.66×10^{-1}
80.0	2	2.55×10^{-3}
80.0	3	1.45×10^{-4}
80.0	4	1.00×10^{-8}
90.0	1	4.64×10^{-1}
90.0	2	2.55×10^{-3}
90.0	3	1.63×10^{-4}
90.0	4	1.12×10^{-8}
100.0	1	4.63×10^{-1}
100.0	2	2.55×10^{-3}
100.0	3	1.80×10^{-4}
100.0	4	1.23×10^{-8}

7.3 Newton iterations per time step — Exam Task (linear bimetallic case)

Table 5: Newton iterations and final residual at each time step.

Time t (s)	Newton iters	Final residual
0.1	1	1.15×10^{4}
0.1	2	1.39×10^{-4}
0.1	3	1.52×10^{-11}
0.2	1	5.48×10^{2}
0.2	2	3.44×10^{-6}
0.2	3	2.05×10^{-12}
0.3	1	5.44×10^{2}
0.3	2	3.90×10^{-6}
0.3	3	2.63×10^{-12}
0.4	1	5.42×10^{2}
0.4	2	1.20×10^{-5}
0.4	3	2.77×10^{-12}
0.5	1	5.40×10^{2}
0.5	2	3.33×10^{-6}
0.5	3	2.77×10^{-12}
0.6	1	5.38×10^{2}
0.6	2	5.03×10^{-6}
0.6	3	3.98×10^{-12}
0.7	1	5.37×10^{2}
0.7	2	6.22×10^{-7}
0.8	1	5.36×10^{2}
0.8	2	6.60×10^{-6}
0.8	3	4.20×10^{-12}
0.9	1	5.34×10^{2}
0.9	2	2.90×10^{-6}
0.9	3	4.68×10^{-12}
1.0	1	5.33×10^{2}
1.0	2	9.14×10^{-6}
1.0	3	3.66×10^{-12}
1.1	1	5.32×10^{2}
1.1	2	2.96×10^{-6}
1.1	3	4.68×10^{-12}
1.2	1	5.31×10^{2}
1.2	2	1.48×10^{-6}
1.2	3	5.37×10^{-12}
1.3	1	5.30×10^{2}
1.3	2	2.87×10^{-6}
1.3	3	5.31×10^{-12}
1.4	1	5.29×10^{2}
1.4	2	2.64×10^{-6}
1.4	3	5.05×10^{-12}
1.5	1	5.28×10^{2}
1.5	2	3.00×10^{-6}
1.5	3	6.32×10^{-12}
1.6	1	5.27×10^{2}
1.6	2	2.05×10^{-6}
1.6	3	7.77×10^{-12}
1.7	1	5.26×10^{2}
1.7	2	4.27×10^{-6}
1.7	3	6.34×10^{-12}
1.8	1	5.25×10^{2}
1.8	2	8.07×10^{-6}
1.8	3	7.25×10^{-12}
1.9	1	5.24×10^{2}

Continued on next page

Time t (s)	Newton iters	Final residual
1.9	2	7.97×10^{-6}
1.9	3	1.27×10^{-11}
2.0	1	5.23×10^{2}
2.0	2	2.65×10^{-6}
2.0	3	9.98×10^{-12}
2.1	1	5.22×10^{2}
2.1	2	4.23×10^{-6}
2.1	3	7.82×10^{-12}
2.2	1	5.22×10^{2}
2.2	2	4.12×10^{-6}
2.2	3	8.72×10^{-12}
2.3	1	5.21×10^{2}
2.3	2	5.66×10^{-6}
2.3	3	1.06×10^{-11}
2.4	1	5.20×10^{2}
2.4	2	5.33×10^{-6}
2.4	3	1.18×10^{-11}
2.5	1	5.19×10^{2}
2.5	2	1.65×10^{-6}
2.5	3	7.90×10^{-12}
2.6	1	5.18×10^{2}
2.6	2	8.76×10^{-6}
2.6	3	1.77×10^{-11}
2.7	1	5.18×10^{2}
2.7	2	1.81×10^{-6}
2.7	3	1.38×10^{-11}
2.8	1	5.17×10^{2}
2.8	2	6.76×10^{-7}
2.9	1	5.16×10^{2}
2.9	2	2.65×10^{-6}
2.9	3	1.12×10^{-11}
3.0	1	5.16×10^{2}
3.0	2	6.81×10^{-6}
3.0	3	1.27×10^{-11}
3.1	1	5.15×10^{2}
3.1	2	2.07×10^{-6}
3.1	3	1.79×10^{-11}
3.2	1	5.14×10^{2}
3.2	2	2.29×10^{-6}
3.2	3	1.47×10^{-11}
3.3	1	5.14×10^{2}
3.3	2	2.25×10^{-6}
3.3	3	1.51×10^{-11}
3.4	1	5.13×10^{2}
3.4	2	4.29×10^{-6}
3.4	3	1.48×10^{-11}
3.5	1	5.12×10^{2}
3.5	2	2.41×10^{-6}
3.5	3	2.09×10^{-11}
3.6	1	5.12×10^{2}
3.6	2	4.38×10^{-6}
3.6	3	1.19×10^{-11}
3.7	1	5.11×10^{2}
3.7	2	4.31×10^{-6}
3.7	3	1.60×10^{-11}
3.8	1	5.10×10^{2}
3.8	2	1.19×10^{-6}
3.8	3	2.16×10^{-11}

Continued on next page

Time t (s)	Newton iters	Final residual
3.9	1	5.10×10^{2}
3.9	2	2.15×10^{-6}
3.9	3	1.65×10^{-11}
4.0	1	5.09×10^{2}
4.0	2	7.24×10^{-6}
4.0	3	1.82×10^{-11}
4.1	1	5.08×10^{2}
4.1	2	8.00×10^{-6}
4.1	3	1.63×10^{-11}
4.2	1	5.08×10^{2}
4.2	2	2.89×10^{-6}
4.2	3	2.04×10^{-11}
4.3	1	5.07×10^{2}
4.3	2	2.19×10^{-6}
4.3	3	1.85×10^{-11}
4.4	1	5.07×10^{2}
4.4	2	9.44×10^{-7}
4.5	1	5.06×10^{2}
4.5	2	2.60×10^{-6}
4.5	3	2.92×10^{-11}
4.6	1	5.06×10^{2}
4.6	2	2.15×10^{-6}
4.6	3	2.57×10^{-11}
4.7	1	5.05×10^{2}
4.7	2	4.99×10^{-7}
4.8	1	5.04×10^{2}
4.8	2	1.34×10^{-6}
4.8	3	1.52×10^{-11}
4.9	1	5.04×10^{2}
4.9	2	7.52×10^{-6}
4.9	3	2.65×10^{-11}
5.0	1	5.03×10^{2}
5.0	2	1.02×10^{-6}
5.0	3	2.04×10^{-11}

7.4 Newton iterations per time step — Exam Task (nonlinear bimetallic case)

Table 6: Newton iterations and residuals at each time step.

Time t (s)	Iteration	Residual
0.1	1	1.15×10^{4}
0.1	2	1.47×10^{1}
0.1	3	6.18×10^{-1}
0.1	4	1.29
0.1	5	5.44×10^{-2}
0.1	6	3.41×10^{-4}
0.1	7	1.07×10^{-5}
0.1	8	1.26×10^{-8}
0.2	1	5.47×10^{2}
0.2	2	8.43×10^{-1}
0.2	3	6.01×10^{-3}
0.2	4	1.03×10^{-4}
0.2	5	6.42×10^{-8}
0.3	1	5.43×10^{2}
0.3	2	9.11×10^{-1}
0.3	3	6.96×10^{-3}
0.3	4	2.18×10^{-4}
0.3	5	7.95×10^{-8}
0.4	1	5.41×10^{2}
0.4	2	9.22×10^{-1}
0.4	3	7.10×10^{-3}
0.4	4	2.24×10^{-4}
0.4	5	7.69×10^{-8}
0.5	1	5.38×10^{2}
0.5	2	9.24×10^{-1}
0.5	3	7.11×10^{-3}
0.5	4	2.17×10^{-4}
0.5	5	7.11×10^{-8}
0.6	1	5.36×10^{2}
0.6	2	9.22×10^{-1}
0.6	3	7.06×10^{-3}
0.6	4	2.05×10^{-4}
0.6	5	6.54×10^{-8}
0.7	1	5.34×10^{2}
0.7	2	9.20×10^{-1}
0.7	3	7.02×10^{-3}
0.7	4	1.94×10^{-4}
0.7	5	6.05×10^{-8}
0.8	1	5.32×10^{2}
0.8	2	9.17×10^{-1}
0.8	3	6.96×10^{-3}
0.8	4	1.82×10^{-4}
0.8	5	5.60×10^{-8}
0.9	1	5.31×10^{2}
0.9	2	9.13×10^{-1}
0.9	3	6.90×10^{-3}
0.9	4	1.70×10^{-4}
0.9	5	5.21×10^{-8}

Time t (s)	Iteration	Residual
1.0	1	5.29×10^{2}
1.0	2	9.10×10^{-1}
1.0	3	6.86×10^{-3}
1.0	4	1.60×10^{-4}
1.0	5	4.88×10^{-8}
1.1	1	5.27×10^{2}
1.1	2	9.06×10^{-1}
1.1	3	6.80×10^{-3}
1.1	4	1.49×10^{-4}
1.1	5	4.57×10^{-8}
1.2	1	5.26×10^{2}
1.2	2	9.02×10^{-1}
1.2	3	6.75×10^{-3}
1.2	4	1.39×10^{-4}
1.2	5	4.29×10^{-8}
1.3	1	5.24×10^{2}
1.3	2	8.98×10^{-1}
1.3	3	6.70×10^{-3}
1.3	4	1.28×10^{-4}
1.3	5	4.04×10^{-8}
1.4	1	5.23×10^{2}
1.4	2	8.94×10^{-1}
1.4	3	6.66×10^{-3}
1.4	4	1.18×10^{-4}
1.4	5	3.81×10^{-8}
1.5	1	5.21×10^{2}
1.5	2	8.90×10^{-1}
1.5	3	6.61×10^{-3}
1.5	4	1.07×10^{-4}
1.5	5	3.61×10^{-8}
1.6	1	5.20×10^{2}
1.6	2	8.86×10^{-1}
1.6	3	6.57×10^{-3}
1.6	4	9.73×10^{-5}
1.6	5	3.42×10^{-8}
1.7	1	5.18×10^{2}
1.7	2	8.82×10^{-1}
1.7	3	6.54×10^{-3}
1.7	4	8.71×10^{-5}
1.7	5	3.26×10^{-8}
1.8	1	5.17×10^{2}
1.8	2	8.78×10^{-1}
1.8	3	6.50×10^{-3}
1.8	4	7.81×10^{-5}
1.8	5	3.11×10^{-8}
1.9	1	5.16×10^{2}
1.9	2	8.74×10^{-1}
1.9	3	6.47×10^{-3}
1.9	4	6.84×10^{-5}
1.9	5	2.98×10^{-8}
2.0	1	5.14×10^{2}
2.0	2	8.70×10^{-1}
2.0	3	6.45×10^{-3}
2.0	4	5.90×10^{-5}
2.0	5	2.90×10^{-8}
2.1	1	5.13×10^{2}
2.1	2	8.66×10^{-1}
2.1	3	6.42×10^{-3}

Continued on next page

Time t (s)	Iteration	Residual
2.1	4	5.04×10^{-5}
2.1	5	2.85×10^{-8}
2.2	1	5.12×10^{2}
2.2	2	8.63×10^{-1}
2.2	3	6.41×10^{-3}
2.2	4	4.27×10^{-5}
2.2	5	2.85×10^{-8}
2.3	1	5.11×10^{2}
2.3	2	8.59×10^{-1}
2.3	3	6.39×10^{-3}
2.3	4	3.60×10^{-5}
2.3	5	2.95×10^{-8}
2.4	1	5.10×10^{2}
2.4	2	8.55×10^{-1}
2.4	3	6.38×10^{-3}
2.4	4	3.13×10^{-5}
2.4	5	3.13×10^{-8}
2.5	1	5.08×10^{2}
2.5	2	8.51×10^{-1}
2.5	3	6.38×10^{-3}
2.5	4	2.95×10^{-5}
2.5	5	3.46×10^{-8}
2.6	1	5.07×10^{2}
2.6	2	8.47×10^{-1}
2.6	3	6.38×10^{-3}
2.6	4	3.09×10^{-5}
2.6	5	3.82×10^{-8}
2.7	1	5.06×10^{2}
2.7	2	8.44×10^{-1}
2.7	3	6.38×10^{-3}
2.7	4	3.50×10^{-5}
2.7	5	4.32×10^{-8}
2.8	1	5.05×10^{2}
2.8	2	8.40×10^{-1}
2.8	3	6.40×10^{-3}
2.8	4	4.18×10^{-5}
2.8	5	4.99×10^{-8}
2.9	1	5.04×10^{2}
2.9	2	8.36×10^{-1}
2.9	3	6.40×10^{-3}
2.9	4	4.82×10^{-5}
2.9	5	5.64×10^{-8}
3.0	1	5.03×10^{2}
3.0	2	8.33×10^{-1}
3.0	3	6.43×10^{-3}
3.0	4	5.69×10^{-5}
3.0	5	6.53×10^{-8}
3.1	1	5.02×10^{2}
3.1	2	8.29×10^{-1}
3.1	3	6.45×10^{-3}
3.1	4	6.60×10^{-5}
3.1	5	7.51×10^{-8}
3.2	1	5.00×10^{2}
3.2	2	8.26×10^{-1}
3.2	3	6.48×10^{-3}
3.2	4	7.53×10^{-5}
3.2	5	8.61×10^{-8}
3.3	1	4.99×10^{2}

Continued on next page

Time t (s)	Iteration	Residual
3.3	2	8.22×10^{-1}
3.3	3	6.51×10^{-3}
3.3	4	8.44×10^{-5}
3.3	5	9.77×10^{-8}
3.4	1	4.98×10^{2}
3.4	2	8.19×10^{-1}
3.4	3	6.54×10^{-3}
3.4	4	9.29×10^{-5}
3.4	5	1.10×10^{-7}
3.5	1	4.97×10^{2}
3.5	2	8.15×10^{-1}
3.5	3	6.59×10^{-3}
3.5	4	1.03×10^{-4}
3.5	5	1.25×10^{-7}
3.6	1	4.96×10^{2}
3.6	2	8.12×10^{-1}
3.6	3	6.64×10^{-3}
3.6	4	1.13×10^{-4}
3.6	5	1.40×10^{-7}
3.7	1	4.95×10^{2}
3.7	2	8.09×10^{-1}
3.7	3	6.69×10^{-3}
3.7	4	1.23×10^{-4}
3.7	5	1.57×10^{-7}
3.8	1	4.94×10^{2}
3.8	2	8.05×10^{-1}
3.8	3	6.74×10^{-3}
3.8	4	1.32×10^{-4}
3.8	5	1.73×10^{-7}
3.9	1	4.93×10^{2}
3.9	2	8.02×10^{-1}
3.9	3	6.80×10^{-3}
3.9	4	1.42×10^{-4}
3.9	5	1.92×10^{-7}
4.0	1	4.92×10^{2}
4.0	2	7.99×10^{-1}
4.0	3	6.86×10^{-3}
4.0	4	1.51×10^{-4}
4.0	5	2.12×10^{-7}
4.1	1	4.91×10^{2}
4.1	2	7.96×10^{-1}
4.1	3	6.93×10^{-3}
4.1	4	1.61×10^{-4}
4.1	5	2.33×10^{-7}
4.2	1	4.90×10^{2}
4.2	2	7.93×10^{-1}
4.2	3	7.00×10^{-3}
4.2	4	1.71×10^{-4}
4.2	5	2.57×10^{-7}
4.3	1	4.89×10^{2}
4.3	2	7.89×10^{-1}
4.3	3	7.08×10^{-3}
4.3	4	1.81×10^{-4}
4.3	5	2.80×10^{-7}
4.4	1	4.88×10^{2}
4.4	2	7.86×10^{-1}
4.4	3	7.16×10^{-3}
4.4	4	1.92×10^{-4}

Continued on next page

Time t (s)	Iteration	Residual
4.4	5	3.06×10^{-7}
4.5	1	4.87×10^{2}
4.5	2	7.83×10^{-1}
4.5	3	7.24×10^{-3}
4.5	4	2.01×10^{-4}
4.5	5	3.33×10^{-7}
4.6	1	4.86×10^{2}
4.6	2	7.80×10^{-1}
4.6	3	7.33×10^{-3}
4.6	4	2.12×10^{-4}
4.6	5	3.61×10^{-7}
4.7	1	4.86×10^{2}
4.7	2	7.77×10^{-1}
4.7	3	7.41×10^{-3}
4.7	4	2.22×10^{-4}
4.7	5	3.92×10^{-7}
4.8	1	4.85×10^{2}
4.8	2	7.74×10^{-1}
4.8	3	7.50×10^{-3}
4.8	4	2.32×10^{-4}
4.8	5	4.21×10^{-7}
4.9	1	4.84×10^{2}
4.9	2	7.71×10^{-1}
4.9	3	7.60×10^{-3}
4.9	4	2.42×10^{-4}
4.9	5	4.55×10^{-7}
5.0	1	4.83×10^{2}
5.0	2	7.68×10^{-1}
5.0	3	7.69×10^{-3}
5.0	4	2.52×10^{-4}
5.0	5	4.89×10^{-7}

Formatting notes: times are rounded to one decimal for display; residuals are shown in scientific notation with three significant figures via `siunitx`. The iteration count equals the number of Newton steps listed in your log for each time.